

Electronic structure of tris(8-hydroxyquinolinato)aluminium(III) revisited using the Heyd-Scuseria-Ernzerhof hybrid functional: Theory and experiments

F. Bisti,^{1,*} A. Stroppa,² M. Donarelli,¹ S. Picozzi,² and L. Ottaviano^{1,2}

¹*Dipartimento di Fisica, Università dell'Aquila, Via Vetoio 10, I-67100 L'Aquila, Italy*

²*CNR-SPIN L'Aquila, Via Vetoio 10, I-67100 L'Aquila, Italy*

(Received 16 September 2011; published 9 November 2011)

The electronic properties of tris(8-hydroxyquinolinato)aluminium(III) (AlQ₃) have been revisited using the screened hybrid Heyd-Scuseria-Ernzerhof density functional theory. We show that such approach very well accounts for the experimental occupied (valence band spectrum) and unoccupied (inverse photoemission spectrum) states. Furthermore, the density of states projected onto nitrogen, oxygen, and carbon are compared with soft x-ray adsorption and emission spectroscopy, showing a very good agreement between theory and experiments. Finally, a fully theoretical interpretation of the carbon 1s core level is proposed.

DOI: [10.1103/PhysRevB.84.195112](https://doi.org/10.1103/PhysRevB.84.195112)

PACS number(s): 71.15.Ap, 71.20.Rv

I. INTRODUCTION

Tris(8-hydroxyquinolinato)aluminium(III) (AlQ₃) is one of the most studied organic molecules, due to its application as an active layer in OLED systems¹ and, recently, as a nonmagnetic conducting layer in spin valves.² Many theoretical and experimental works have been performed in order to investigate the electronic structure of this material.^{3–14} In particular, the knowledge of the electronic structure is very important for studying the interaction of the AlQ₃ molecule at the interface with different substrates,^{15,16} or to modify its properties with dopant atoms.¹⁷

The electronic structure of AlQ₃ was firstly calculated using density functional theory (DFT) under the generalized gradient approximations (GGA) some years ago by Curioni *et al.*³ Besides a comparison with valence band spectroscopy experiments, the DFT calculations were also used to interpret soft x-ray absorption spectroscopy (XAS) experiments³ and soft x-ray emission spectroscopy (XES) spectra.⁵ In both cases a detailed knowledge of the core level electronic energy of inequivalent atoms is required, either from experiments (core level photoemission)⁵ or from DFT.³

The exchange-correlation functionals in the local and semilocal approximations allow for a spurious interaction of an electron with itself.¹⁸ This error is better known as self-interaction error (SIE) and the more localized the electron state, the higher the SIE.¹⁹ Especially for organic systems, due to SIE, the calculated GGA density of states (DOS) usually does not match the experimental valence band photoemission.¹⁹ Sometimes a phenomenological parameter (“stretch factor”) is introduced to rescale the obtained energy eigenvalues to find the best agreement with experiments (valence band photoemission spectra).²⁰ Unfortunately, in many cases, a substantial disagreement between theory and experiments still remains, due to the intrinsic inaccuracy of the theoretical approximations.^{19,20} A possible way out is to go beyond standard GGA DFT calculations by introducing a hybrid Hartree-Fock density functional.^{21–24} Hybrid functionals mix the exact nonlocal exchange of Hartree-Fock theory^{21–24} with the density functional exchange; this treatment has the advantage of reducing the SIE.¹⁸ A popular choice for the hybrid functional is the semiempirical B3LYP²⁵ which has been also applied to AlQ₃ for calculating accurately the molecular

structure^{26,27} and the energy gap.²⁸ More recently, the Heyd-Scuseria-Ernzerhof screened hybrid functional (HSE)^{29,30} has been introduced and widely used in many different systems, ranging from simple semiconductor systems, to transition metals, lanthanides, actinides, molecules at surfaces, diluted magnetic semiconductors, and carbon nanostructures (for a recent review see Ref. 31). We have recently applied DFT HSE calculation to an interesting ferroelectric organic crystal, such as the croconic acid, showing an excellent agreement between theory and experiments.³²

In this work, the valence DOS and the core levels of AlQ₃ atoms were calculated using HSE and compared to AlQ₃ thermal evaporated thin film valence band and core level photoemission spectra probed by laboratory sources. Furthermore, the calculated unoccupied states were compared using inverse photoemission spectroscopy (IPES) data reported by different authors.^{10,11} We have found a very good agreement between theory and experiments as far as the photoemission and inverse photoemission spectrum peak energies are concerned. A theoretical explanation of the C 1s core level is also proposed, which differs from the one reported in the literature.⁶ Finally, the HSE projected DOS (PDOS) onto *p* states were corrected by core level shifts (CLS) for carbon, nitrogen, and oxygen for interpreting the XAS and XES experimental data of De Masi *et al.*⁵ A comparison with the existing literature is also considered.^{3,5}

II. EXPERIMENT

AlQ₃ (Sigma-Aldrich, 99.995%, 459.43 molecular weight) was deposited by vacuum thermal evaporation, from a quartz crucible held in an ultrahigh vacuum chamber (base pressure equal to 10⁻¹⁰ Torr) on silicon oxide substrates. The deposition rate was 0.3 Å/s (as monitored *in situ* by a quartz crystal microbalance). The electronic structure of the AlQ₃ film was studied by x-ray photoemission spectroscopy (XPS) (PHI 1257 spectrometer, monochromatic Al K α source, $h\nu = 1486.6$ eV) and ultraviolet photoemission spectroscopy (UPS) (PHI 1257 spectrometer, He discharge lamp source, $h\nu = 21.2$ eV He I, $h\nu = 40.8$ eV He II). The core level spectra were acquired with a pass energy of 11.75 eV and a corresponding overall experimental resolution of 0.25 eV. The overall UPS spectral

resolution was estimated to be 0.1 eV from the Fermi edge width, at room temperature, of a thermally cleaned gold substrate. Voigt line shapes and a Shirley background were used to fit the spectra. An asymmetric Doniach-Sunjić convoluted with a Gaussian was used only for the shake-up component in the C 1s spectrum. DFT calculations were performed using the Vienna *Ab-initio* Simulation Package (VASP)³³ for the isolated AlQ₃ mer-isomer (mer-AlQ₃). A plane-wave cutoff of 400 eV with the Γ point only has been used. For the exchange-correlation functional, we used the HSE hybrid functional^{29,30,34} and, for comparison, the Perdew-Burke-Ernzerhof (PBE) generalized gradient approximation (GGA) functional.^{35,36} The atomic positions were relaxed until the Hellman-Feynman forces were <0.02 eV/Å. The core level energies were calculated in the final-state approximation.³⁷ For comparison with experiments, the calculated Kohn-Sham discrete levels were broadened using a Gaussian function with $\sigma = 0.3$ eV in the case of photoemission and inverse photoemission spectra, and with $\sigma = 0.4$ eV for XAS and XES.

III. RESULTS AND DISCUSSION

In Fig. 1(a) (from top to bottom), we report the SXPS experimental data and the GGA calculations of Curioni *et al.*,³ the UPS He I and He II valence band of 60 nm AlQ₃/SiO₂, and the HSE DFT calculated DOS. The HSE DFT calculated PDOS for each atom type are reported in Fig. 1(b). The experimental data (ours and from Ref. 3) are very similar,

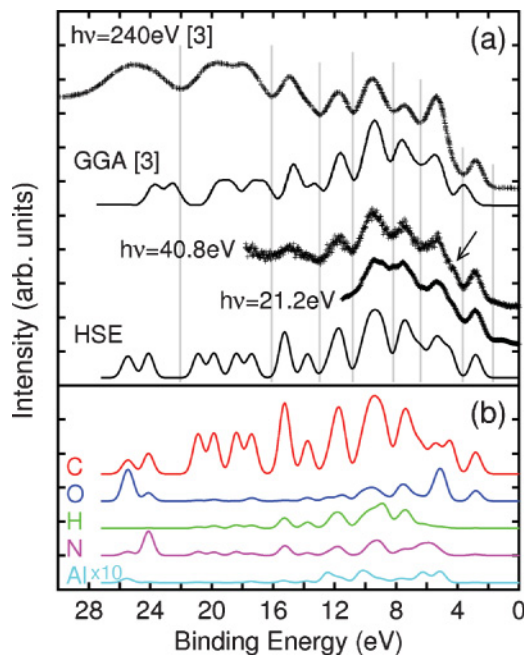


FIG. 1. (Color online) AlQ₃ valence band photoemission spectra at 240 eV photon energy (Ref. 3) and 60 nm AlQ₃/SiO₂ at 40.8 eV and at 21.2 eV, compared with GGA (Ref. 3) and HSE DFT calculations. Crosses, experimental data. Black lines, total density of states calculated by DFT. Red, blue, green, magenta, and cyan lines, total carbon, oxygen, hydrogen, nitrogen, and aluminium projected density of states, respectively (also see labels). Arrow points to the shoulder of the second HOMO peak (see text).

apart from slight changes due to the different photon energy cross section (mostly visible in the 4–7 eV energy range). The GGA calculations from Curioni *et al.*³ match the experimental energy peak positions in the 4–16 eV energy range. At higher binding energies the agreement is worse and, most importantly, there is a substantial disagreement in the position of the energy peak of the HOMO (highest occupied molecular orbital). On the other hand, the HSE calculated DOS is in very good agreement with experimental data in the whole energy range. The binding energy of the HOMO is perfectly aligned with the experimental one. Note the presence of a shoulder at low energy of the second HOMO peak (at 4.5 eV, shown by the arrow) (already observed by different authors^{6,17}), visible at 21.2 eV and 40.8 eV photon energies, correctly reproduced by HSE but not by GGA calculations. This shoulder is due to the presence of two DOS peaks of mainly C 2p and O 2p character in the same energy region. While the GGA put them at almost the same energy position (not shown here), the HSE shifts the O 2p peak at higher binding energy due to the self-interaction correction giving rise to the shoulder in the total DOS, thus revealing the “fine” structure at 4.5 eV. However, the same shoulder disappears with 240 eV photon energy. This is probably due to cross-section effects: With higher photon energy, the weight associated with the O 2p orbital increases, due to the increase of the cross section of these orbitals with respect to the C 2p ones, thus destroying the “fine” structure in this energy region.

In Fig. 2, we report the comparison between the IPES data and the calculated unoccupied states using HSE and PBE-GGA functionals. The experimental data of Ref. 10 and the theoretical calculations are aligned to the curve fit of Ref. 11. In this case, both functionals show good agreement with experimental data. This means that the considered unoccupied states are not so much affected by SIE and this is consistent with their lower spatial localization.¹⁹

Figure 3 (top panel) reports the AlQ₃ C 1s core level spectrum. The core level spectra of nitrogen, oxygen, and aluminium are not reported for brevity, since the peak shapes are similar to those observed by Pi *et al.*⁶ The spectrum has been fitted with nine identical components (labelled as 1–9) having the same Voigt shapes and intensities, plus one shake-up satellite (labelled as 10). The components were

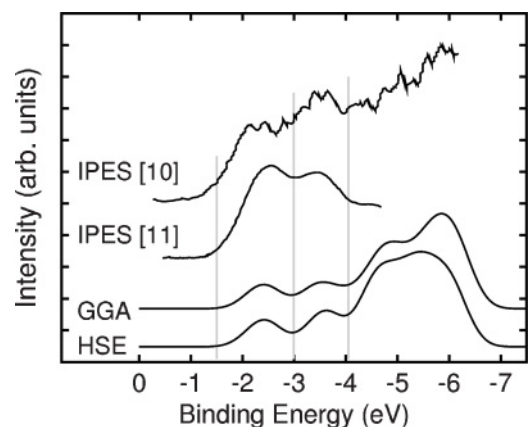


FIG. 2. AlQ₃ IPES of Ref. 10 and IPES curve fit of Ref. 11 compared with PBE-GGA and HSE DFT calculations.

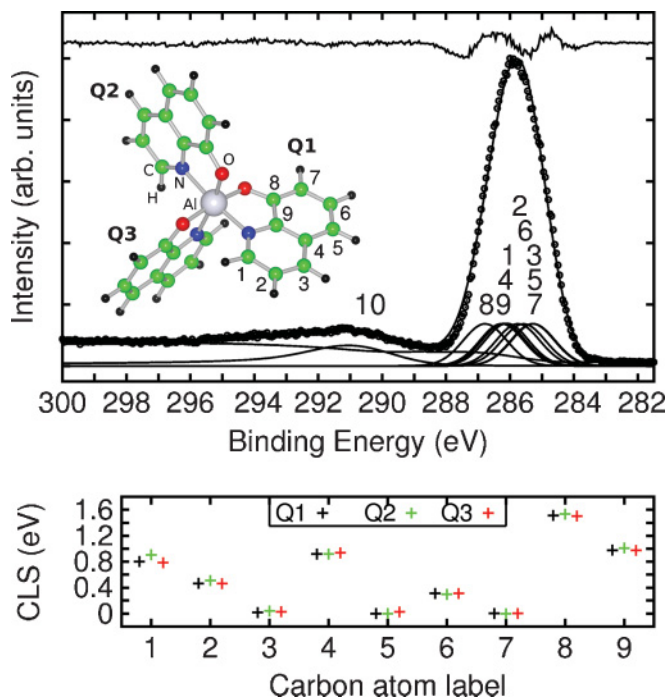


FIG. 3. (Color online) Top panel: AlQ_3 C $1s$ core level spectrum (from 60 nm $\text{AlQ}_3/\text{SiO}_2$). Dots: experimental data. Solid curves: HSE DFT calculations in the final-state approximation for the isolated molecule. Inset top panel: molecular structure of AlQ_3 . Bottom panel: core level shifts of each (27) carbon atom in the molecule; the labeling is consistent with the molecular scheme in the top panel.

considered corresponding to the nine different carbon atoms of each 8-hydroxyquinoline ligand (Q). The core level peak energies of these components were constrained to the mean values of the corresponding Q1, Q2, and Q3 DFT calculated values (reported in the bottom panel of Fig. 3) after offset correction.^{38,39} All the above constraints limit the fitting degrees of freedom essentially to just two parameters (peak intensity and width) yielding a remarkable agreement between theory and experiment.

Going into details of this C $1s$ core level decomposition, considering only one ligand, from higher to lower binding energies there are the carbon atom near the oxygen (8), then the carbons near the nitrogen (1, 9) but also the carbon surrounded by carbons (4), and finally the carbons bonded with hydrogens (2, 6, 3, 5, 7). In our approach, the most important differences with respect to the interpretation of Pi *et al.*⁶ (three components fitting procedure, based on the first-nearest-neighbor atoms of each carbon atom in the molecule) are: (i) in our case, peak 4 is not assigned to the lowest binding energy component of the spectrum, meaning that the corresponding carbon atom, even if surrounded by other carbons, does not screen the core level more than the carbons bonded to hydrogen do; (ii) the core level binding energy of the carbon near oxygen (8) is not degenerate with those of carbons bound with nitrogen (1, 9). Furthermore, based on our calculations, we can also see slight differences in the core level energies of corresponding atoms belonging to different ligand groups (Q1, Q2, Q3). In particular (see Fig. 3) the main differences are in the 1 and 2,

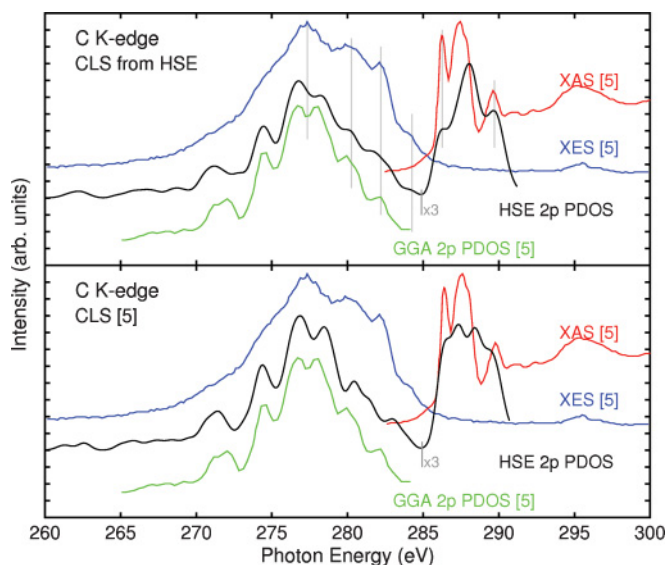


FIG. 4. (Color online) C K-edge XAS spectra (red lines), XES spectra (blue lines), and theoretical p -orbital PDOS calculations from De Masi *et al.* (Ref. 5) (green lines) compared with HSE p -orbital PDOS corrected by HSE calculated CLS (top panel, black line) and corrected by the same CLS of De Masi *et al.* (Ref. 5) (bottom panel, black line). In each panel, HSE unoccupied p -orbital PDOS is vertically magnified by a factor of 3 for clarity.

and those are due to the different distance of the ligands (Q1, Q2, Q3) from the Al^{3+} ion.

After benchmarking our calculations with experimental valence band spectra, we can interpret the experimental XAS and XES spectra⁵ where De Masi *et al.* used GGA DFT calculations and CLS obtained from experiment⁶ for the interpretation of the spectra. Here we propose a fully theoretical explanation based on HSE calculations of PDOS and the CLS.

The XAS (XES) mechanism is based on the photon absorption (emission) due to a transition of an electron localized at an atomic core level (valence band level) to an unoccupied conduction band state (hole localized in an atomic core level). Since an electronic transition, in the dipole approximation, is governed by selection rules ($\Delta l_{el} = \pm 1$), XAS (XES) in a good approximation probes the unoccupied (occupied) PDOS of a specific atomic type. For this reason, these two techniques are very interesting for electronic structure investigations because they probe the projected orbital angular momentum, both occupied and unoccupied (which can be compared with angular resolved PDOS). It is also worthwhile to stress that, since in both cases (XAS, XES) the electronic transition involves an atomic core level, the CLS of the different atoms are needed to reliably reproduce the spectra.⁵

In Figs. 4 and 5, we show the C, N, O K-edge XES and XAS spectra;⁵ the GGA DFT calculations by De Masi *et al.*;⁵ and our HSE DFT calculated p -orbital PDOS corrected by different types of CLS. The occupied HSE PDOS were energetically shifted to match the XES spectra, and then the XAS spectra were shifted to match the unoccupied HSE PDOS. In Fig. 4 (top panel), the C K-edge XES and XAS spectra are compared with the HSE calculated C p -orbital

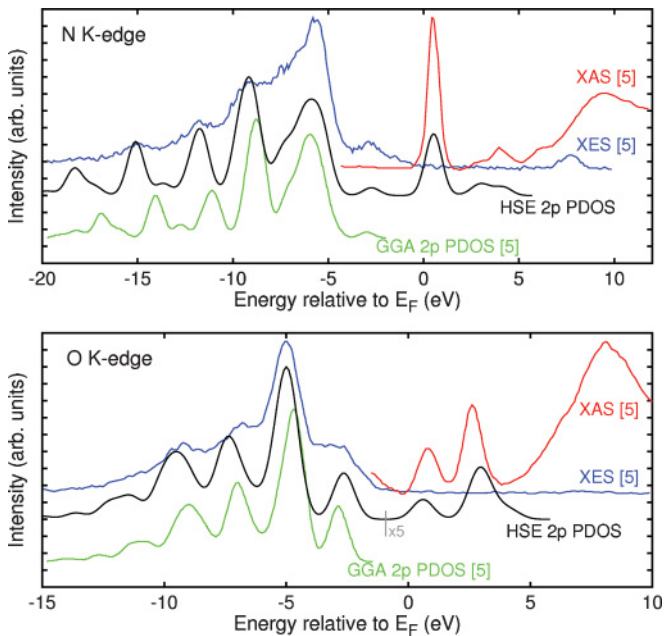


FIG. 5. (Color online) Top (Bottom) panel: N (O) K-edge XAS, red line; XES, blue line; compared with theoretical p -orbital PDOS for nitrogen (oxygen). Green lines, PDOS calculated by GGA (Ref. 5); black lines, PDOS calculated by HSE (for clarity unoccupied oxygen PDOS is vertically magnified by a factor of 5).

PDOS corrected by HSE $C 1s$ CLS; the agreement between experiments and theory is very good in terms of number and energy separation of the peaks. Concerning the XES spectrum, we stress that our calculations match the lower energy peak at 284.5 eV while the GGA calculations corrected by the CLS of Pi *et al.*⁶ do not. In our calculations, this peak is mainly made up by the HOMO of the 8 carbon type and the matching is obtained by (i) a good simulation for the HOMO peak (as discussed before); (ii) a different CLS between C8 and C1 or C9. To better visualize the contribution coming from the HSE CLS, in Fig. 4 bottom panel, HSE calculated PDOS were corrected by the CLS of Pi *et al.*⁶ In this case, there is no matching for the XES lower energy peak and the

theoretical interpretation of the XAS spectrum consists of four theoretical peaks instead of three observed experimental ones. Therefore, the HSE calculated CLS play a fundamental role in the comparison between theoretical and experimental spectra.

In Fig. 5 top (bottom) panel, the N (O) K-edge XES and XAS spectra are compared with N (O) p -orbital PDOS corrected by HSE calculated N (O) $1s$ CLS. In this case, the CLS contribution is not so important: The calculated HSE CLS are spread in an energy range lower than 0.1 eV, which is in agreement with the fact that the N $1s$ (O $1s$) core level spectrum can be fitted by just one component. For nitrogen, the HSE calculations match perfectly the experiments, while, considering XES, the GGA calculations match only the first two peaks. For oxygen, the separation energy between the HSE p -orbital PDOS peaks are slightly greater than the observed experimental ones. In any case, the energy matching is better than for GGA calculations, which are in a good agreement only in the lower energy part of the XES spectrum.

As a final remark, we report that the HSE calculated energy HOMO-LUMO gap is 2.82 eV, very close to the experimentally measured optical gap: 2.8 eV⁴⁰ and 2.86 ± 0.01 eV.⁴¹

IV. SUMMARY

To summarize, using the HSE hybrid functional we have shown (i) an excellent agreement in the interpretation of the experimental occupied (valence band photoelectron spectrum) and unoccupied (inverse photoemission spectrum) states, including a rationale for the second HOMO peak shoulder at low binding energy; (ii) a $C 1s$ core level decomposed using only theoretical data; (iii) more insights in the interpretations of the XES and XAS; (iv) a good estimation for the optical gap.

ACKNOWLEDGMENTS

F.B. thanks Sincrotrone Trieste S.C.p.A. for financial support of his Ph.D. fellowship. The research leading to the theoretical results has received funding from the European Research Council (Grant Agreement No. 203523).

*federico.bisti@aquila.infn.it

¹L. S. Hung and C. H. Chen, *Mat. Sci. Eng. R* **39**, 143 (2002).

²W. J. M. Naber, S. Faez, and W. G. v. d. Wiel, *J. Phys. D* **40**, R205 (2007).

³A. Curioni, W. Andreoni, R. Treusch, F. J. Himpsel, E. Haskal, P. Seidler, C. Heske, S. Kakar, T. v. Buuren, and L. J. Terminello, *Appl. Phys. Lett.* **72**, 1575 (1998).

⁴A. Curioni, M. Boero, and W. Andreoni, *Chem. Phys. Lett.* **294**, 263 (1998).

⁵A. DeMasi, L. F. J. Piper, Y. Zhang, I. Reid, S. Wang, K. E. Smith, J. E. Downes, N. Peltekis, C. McGuinness, and A. Matsuura, *J. Chem. Phys.* **129**, 224705 (2008).

⁶T.-W. Pi, T. Yu, C.-P. Ouyang, J.-F. Wen, and H.-L. Hsu, *Phys. Rev. B* **71**, 205310 (2005).

⁷T.-W. Pi, C.-P. Ouyang, T. C. Yu, H. L. Hsu, J.-F. Wen, and J. Hwang, *Appl. Phys. Lett.* **85**, 908 (2004).

⁸T.-W. Pi, H.-H. Lee, H.-H. Lin, and J. Hwang, *J. Appl. Phys.* **101**, 043704 (2007).

⁹T.-W. Pi and T. C. Yu, *Surf. Rev. Lett.* **14**, 377 (2007).

¹⁰I. G. Hill, A. Kahn, J. Cornil, D. A. d. Santos, and J. L. Brédas, *Chem. Phys. Lett.* **317**, 444 (2000).

¹¹A. Krause, J. Paier, and G. E. Scuseria, *New J. Phys.* **10**, 085001 (2008).

¹²N. Johansson, T. Osada, S. Stafström, W. R. Salaneck, V. Parente, D. A. d. Santos, X. Crispin, and J. L. Brédas, *J. Chem. Phys.* **111**, 2157 (1999).

¹³K. Sugiyama, D. Yoshimura, T. Miyamae, T. Miyazaki, H. Ishii, Y. Ouchi, and K. Seki, *J. Appl. Phys.* **83**, 4928 (1998).

- ¹⁴R. Treusch, F. J. Himpsel, S. Kakar, L. J. Terminello, C. Heske, T. v. Buuren, V. V. Dinh, H. W. Lee, K. Pakbaz, G. Fox, and I. Jiménez, *J. Appl. Phys.* **86**, 88 (1999).
- ¹⁵S. Yanagisawa, K. Lee, and Y. Morikawa, *J. Chem. Phys.* **128**, 244704 (2008).
- ¹⁶S. Yanagisawa, I. Hamada, K. Lee, D. C. Langreth, and Y. Morikawa, *Phys. Rev. B* **83**, 235412 (2011).
- ¹⁷T. Schwieger, H. Peisert, M. Knupfer, M. S. Golden, and J. Fink, *Phys. Rev. B* **63**, 165104 (2001).
- ¹⁸B. G. Janesko, T. M. Henderson, and G. E. Scuseria, *PhysChemChemPhys* **11**, 443 (2009).
- ¹⁹T. Körzdörfer, S. Kümmel, N. Marom, and L. Kronik, *Phys. Rev. B* **79**, 201205 (2009).
- ²⁰N. Marom, O. Hod, G. E. Scuseria, and L. Kronik, *J. Chem. Phys.* **128**, 164107 (2008).
- ²¹P. J. Stephens, F. J. Devlin, C. F. Chabalowski, and M. J. Frisch, *J. Phys. Chem.* **98**, 11623 (1994).
- ²²C. Adamo and V. Barone, *J. Chem. Phys.* **110**, 6158 (1999).
- ²³M. Ernzerhof and G. E. Scuseria, *J. Chem. Phys.* **110**, 5029 (1999).
- ²⁴A. V. Krukau, O. A. Vydrov, A. F. Izmaylov, and G. E. Scuseria, *J. Chem. Phys.* **125**, 224106 (2006).
- ²⁵A. D. Becke, *J. Chem. Phys.* **98**, 5648 (1993).
- ²⁶J. Zhang and G. Frenking, *J. Phys. Chem. A* **108**, 10296 (2004).
- ²⁷R. L. Martin, J. D. Kress, I. H. Campbell, and D. L. Smith, *Phys. Rev. B* **61**, 15804 (2000).
- ²⁸M. Amati and F. Lelj, *J. Phys. Chem. A* **107**, 2560 (2003).
- ²⁹J. Heyd, G. E. Scuseria, and M. Ernzerhof, *J. Chem. Phys.* **118**, 8207 (2003).
- ³⁰J. Heyd, G. E. Scuseria, and M. Ernzerhof, *J. Chem. Phys.* **124**, 219906 (2006).
- ³¹B. G. Janesko, T. M. Henderson, and G. E. Scuseria, *PhysChemChemPhys* **11**, 443 (2009).
- ³²F. Bisti, A. Stroppa, S. Picozzi, and L. Ottaviano, *J. Chem. Phys.* **134**, 174505 (2011).
- ³³G. Kresse and J. Furthmüller, *Phys. Rev. B* **54**, 11169 (1996).
- ³⁴M. Marsman, J. Paier, A. Stroppa, and G. Kresse, *J. Phys. Condens. Matter* **20**, 064201 (2008).
- ³⁵J. P. Perdew, K. Burke, and M. Ernzerhof, *Phys. Rev. Lett.* **77**, 3865 (1996).
- ³⁶J. P. Perdew, K. Burke, and M. Ernzerhof, *Phys. Rev. Lett.* **78**, 1396 (1997).
- ³⁷L. Köhler and G. Kresse, *Phys. Rev. B* **70**, 165405 (2004).
- ³⁸We shifted the absolute value of the core levels because, as is well known, the calculation is reliable only as far as the chemical shifts are concerned; the absolute values are not correct due to correlation effects.
- ³⁹We note that (see Fig. 3, bottom panel) the C 1s core level energies are, for each atomic site, almost degenerate (within 0.2 eV) when considering the three ligands (Q1, Q2, Q3). This justifies restricting the number of fitting components to nine (instead of twenty-seven).
- ⁴⁰P. Dalasinski, Z. Lukasiak, M. Wojdyla, M. Rebarz, and W. Bala, *Opt. Mat.* **28**, 98 (2006).
- ⁴¹F. F. Muhammad, A. I. Abdul Hapip, and K. Sulaiman, *J. Organomet. Chem.* **695**, 2526 (2010).